

## Electronic supplementary informations

# Evidencing $((n\text{-C}_4\text{H}_9)_4\text{N})_2[\text{W}_6\text{I}_{14}]$ red-NIR emission and singlet oxygen generation by two photon absorption

Yann Molard,\* Gregory Taupier, Serge Paofai and Stéphane Cordier

yann.molard@univ-rennes1.fr

### Table of Contents

Table of Contents.....	1
Experimental Procedures.....	1
Synthesis and characterizations of $((n\text{-C}_4\text{H}_9)_4\text{N})_2[\text{W}_6\text{I}_{14}]$ .....	2
Supplementary figures.....	2
Time resolved photoluminescence studies.....	3
AQY measurements.....	6
Two-photon emission spectra.....	6
Singlet oxygen generation studies.....	7
References.....	7

### Experimental Procedures

Starting reagents were purchased from Alfa Aesar, Aldrich or Strem. EDX were realized in CMEBA-SCanMAT platform with a JED-2300 equipped with an EDS ITA300 (LA) spectrometer or with a JSM-7100F equipped with an Oxford X-Max spectrometer.

X-ray diffraction single crystal experiment. Suitable crystal for X-ray diffraction single crystal experiment were selected and mounted with a cryoloop on the goniometer head of a D8 Venture diffractometer diffractometer equipped with a (CMOS) PHOTON 100 detector, using Mo-K $\alpha$  radiation ( $\lambda = 0.71073 \text{ \AA}$ , multilayer monochromator) at  $T = 150(2) \text{ K}$ .

Powder X-Ray diffraction experiments. X-Ray powder diffraction (XRPD) data were collected at room temperature using a Bruker D8 Advance two-circle diffractometer ( $\theta$ - $2\theta$  Bragg-Brentano mode) using Cu K $\alpha$  radiation ( $\lambda = 1.54056 \text{ \AA}$ ) equipped with a Ge(111) monochromator and a Lynx Eye detector. The analyses of the diffraction patterns were performed using the FullProf and WinPlotr software packages.<sup>[1]</sup>

All solvent used for photophysical measurements were of spectrometric grade. UV-vis absorption measurements, one photon emission vs excitation maps were recorded on a Horiba Jobin Yvon Duetta spectrophotometer. Deaeration of CH<sub>3</sub>CN was realized by bubbling Ar in the solution for 30 min directly in the measuring cuvette. The absolute quantum yields were measured with a C9920-03 Hamamatsu system. One photon absorption lifetime measurements and TRPL mapping at 296 K were realized using a picosecond laser diode (Jobin Yvon deltadiode, 375 nm) and a Hamamatsu C10910-25 streak camera mounted with a slow single sweep unit. Signals were integrated on the whole emission decay. Fits were calculated using origin software and the goodness of fit judge by the reduced  $\chi^2$  value and residual plot shape.

Emission spectra by two photon or one photon absorption were recorded using a femtosecond laser chain (Ti-Sapphire Chameleon ultra II Coherent + pulse picker + SHG module when needed, pulse duration: 100-130 fs; pulse frequency: 5 MHz) and an Ocean optics QEPro CCD detector with integrating times ranging from 1 to 20s. The excitation beam crossed a lens before arriving on the sample and a short-pass 750 nm filter after the sample to remove the excitation signal and prevent damages on the CCD detector. The power of the beam was measured with a PMD100 console and a S142C integrating sphere sensor from Thorlabs. For solution measurements, the 2PE was recorded perpendicularly to the beam using an optical fiber connected to a CCD detector. Powder samples were deposited on a quartz substrate with an angle of 30° compared to the direction of the optical fiber.

Two-photon absorption cross-section values were evaluated using Rhodamine B as standard with a quantum yield value of 0.5<sup>[2]</sup> (concentration:  $8.12 \cdot 10^{-5} \text{ mol. l}^{-1}$  in MeOH) using  $\sigma_2$  reference values from Makarov *et al.*<sup>[3]</sup>

O<sub>2</sub> (<sup>1</sup> $\Delta_g$ ) emission measurements were realized using either the picosecond laser diode at 375 nm for 1PE or the femtosecond laser chain for 2PE and detected with a Hamamatsu H12397-75 NIR-PMT unit mounted on an IHR3 spectrometer. In this case, the excitation power was kept low enough to avoid any damages on the sample chamber mirrors.

## Synthesis and characterizations of $((n\text{-C}_4\text{H}_9)_4\text{N})_2[\text{W}_6\text{I}_8\text{I}^{18}_6]$

$((n\text{-C}_4\text{H}_9)_4\text{N})_2[\text{W}_6\text{I}_8\text{I}^{18}_6]$  was prepared according to protocols reported in the literature. The synthesis is realized in three steps:

1)  $\text{W}_6\text{Cl}_{12}$  was synthesized by a multistep reaction from the reduction of  $\text{WCl}_6$  (Strem, 99.9%) by metal bismuth (Strem, 99.9%) in a sealed silica container. The extraction of  $[\text{W}_6\text{Cl}_8\text{Cl}_6]^{2-}$  units was performed in HCl acidic solution and led to the formation of crystalline chloro acid  $(\text{H}_3\text{O})_2[\text{W}_6(\mu_3\text{-Cl})_8\text{Cl}_6](\text{OH}_2)_x$  that was thermally decomposed at  $400^\circ\text{C}$  under vacuum in  $\text{W}_6\text{Cl}_{12}$ .<sup>[4]</sup>

2)  $[\text{W}_6\text{I}_8\text{I}^{18}_6]^{2-}$  cluster units were formed by ligand exchange and excision reaction by reacting at  $540^\circ$  for 15 min, in a sealed silica container, the binary  $\text{W}_6\text{Cl}_{12}$  with a 10-fold excess (i.e. moles of I<sup>-</sup> per mole of Cl<sup>-</sup>) of a molten solution of KI (Alfa Aesar, 99.9%) and LiI (Alfa Aesar, 99.9%) (70:30 mol %).<sup>[5]</sup>

3) the resulting crude product was dissolved in ethanol.  $((n\text{-C}_4\text{H}_9)_4\text{N})_2[\text{W}_6\text{I}_8\text{I}^{18}_6]$  was obtained as a precipitate by addition in the solution of a 2 fold excess of  $(n\text{-C}_4\text{H}_9)_4\text{N}^+$  (Aldrich >99%) per  $[\text{W}_6\text{I}_8\text{I}^{18}_6]^{2-}$ .<sup>[6]</sup> After washing with ethanol and drying at  $60^\circ\text{C}$  in an oven, the  $((n\text{-C}_4\text{H}_9)_4\text{N})_2[\text{W}_6\text{I}_8\text{I}^{18}_6]$  precipitate was dissolved in  $\text{CH}_2\text{Cl}_2$ . Single crystals, with size ranging from 0.1 mm to 0.9 mm, were obtained by slow solvent evaporation.

The single crystal X-ray diffraction studies revealed the same structure for  $((n\text{-C}_4\text{H}_9)_4\text{N})_2[\text{W}_6\text{I}_8\text{I}^{18}_6]$  obtained herein than that reported by T.C. Zietlow et al. (Space group  $\text{P}2_1/n$  (No. 14),  $a = 11.553(7) \text{ \AA}$ ,  $b = 11.486(3) \text{ \AA}$ ,  $c = 24.554(13) \text{ \AA}$ ,  $\beta = 96.77(4)^\circ$ ).<sup>[7]</sup> More recently L. Riehl et al. reported the same structure using X-ray powder investigations (space group  $\text{P}2_1/n$  (No. 14),  $a = 11.5768(2) \text{ \AA}$ ,  $b = 11.4916(3) \text{ \AA}$ ,  $c = 24.5672(5) \text{ \AA}$ ,  $\beta = 96.776(2)^\circ$ ).<sup>[8]</sup> Briefly, this structure is built up from  $[\text{W}_6\text{I}_8\text{I}^{18}_6]^{2-}$  discrete cluster units. The charge of the  $[\text{W}_6\text{I}_8\text{I}^{18}_6]^{2-}$  dianion is counterbalanced by two  $(\text{C}_4\text{H}_9)_4\text{N}^+$  cations. Within the structure, layers of clusters units alternate with layers of  $(\text{C}_4\text{H}_9)_4\text{N}^+$  along the  $c$  direction of the unit cell. EDS analysis of heavy atoms agreed with a W: I ratio of 6:14, with no trace of other heavy atom. A powdered sample of  $((n\text{-C}_4\text{H}_9)_4\text{N})_2[\text{W}_6\text{I}_8\text{I}^{18}_6]$  was obtained by grinding 300 mg of single-crystals. X-ray powder pattern of grounded single crystals, as expected, did not revealed the presence of any impurities or the presence of allotropic forms. Optical analyses were then performed on this pure powdered sample.

## Supplementary figures

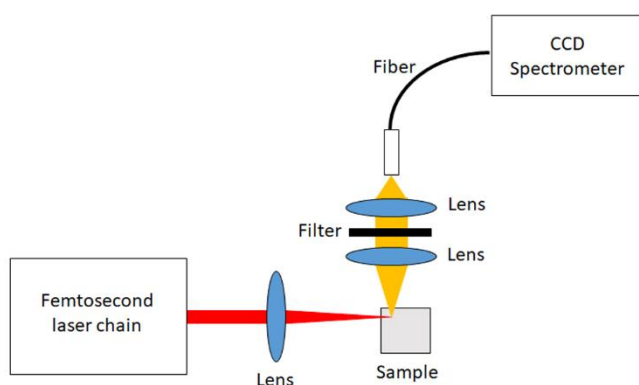


**Figure S1.** Schematic presentation of the photophysical set-up used for two photon absorption induced emission measurements in solution.

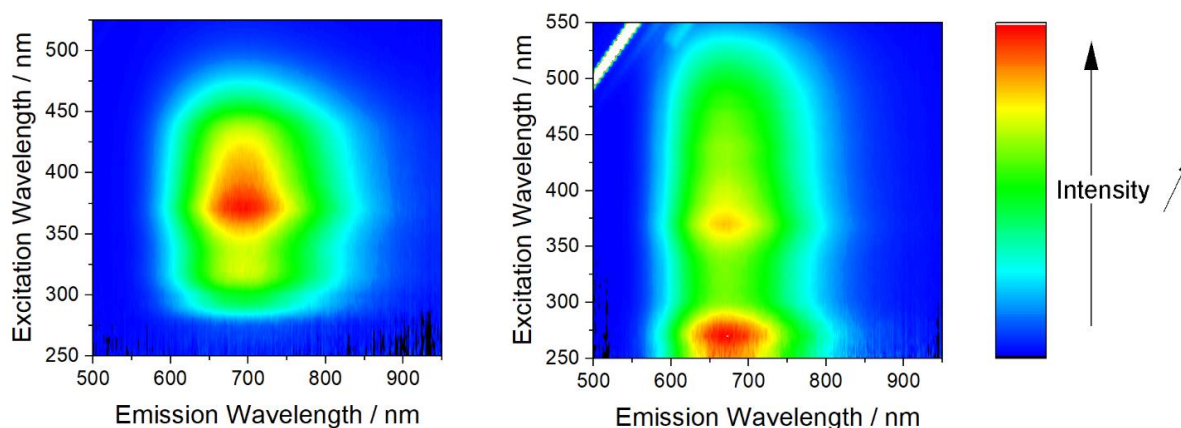


**Figure S2.** Emission vs excitation map of  $((n\text{-C}_4\text{H}_9)_4\text{N})_2[\text{W}_6\text{I}_{14}]$  in  $\text{CH}_3\text{CN}$  (left) and in the solid state (right)

### Time resolved photoluminescence studies

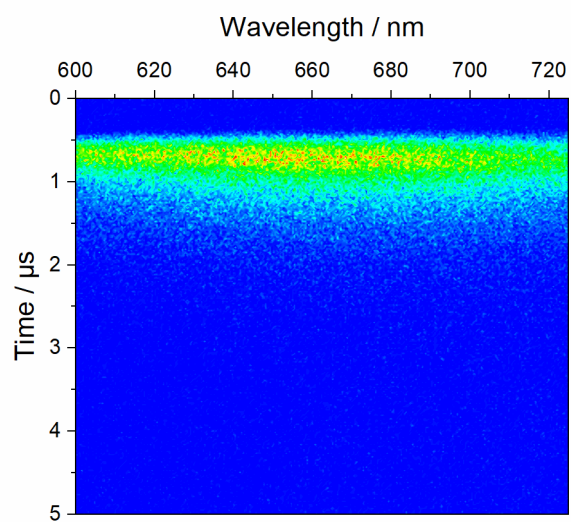


**Figure S3.** Emission decay map of  $((n\text{-C}_4\text{H}_9)_4\text{N})_2[\text{W}_6\text{I}_{14}]$  in aerated  $\text{CH}_3\text{CN}$

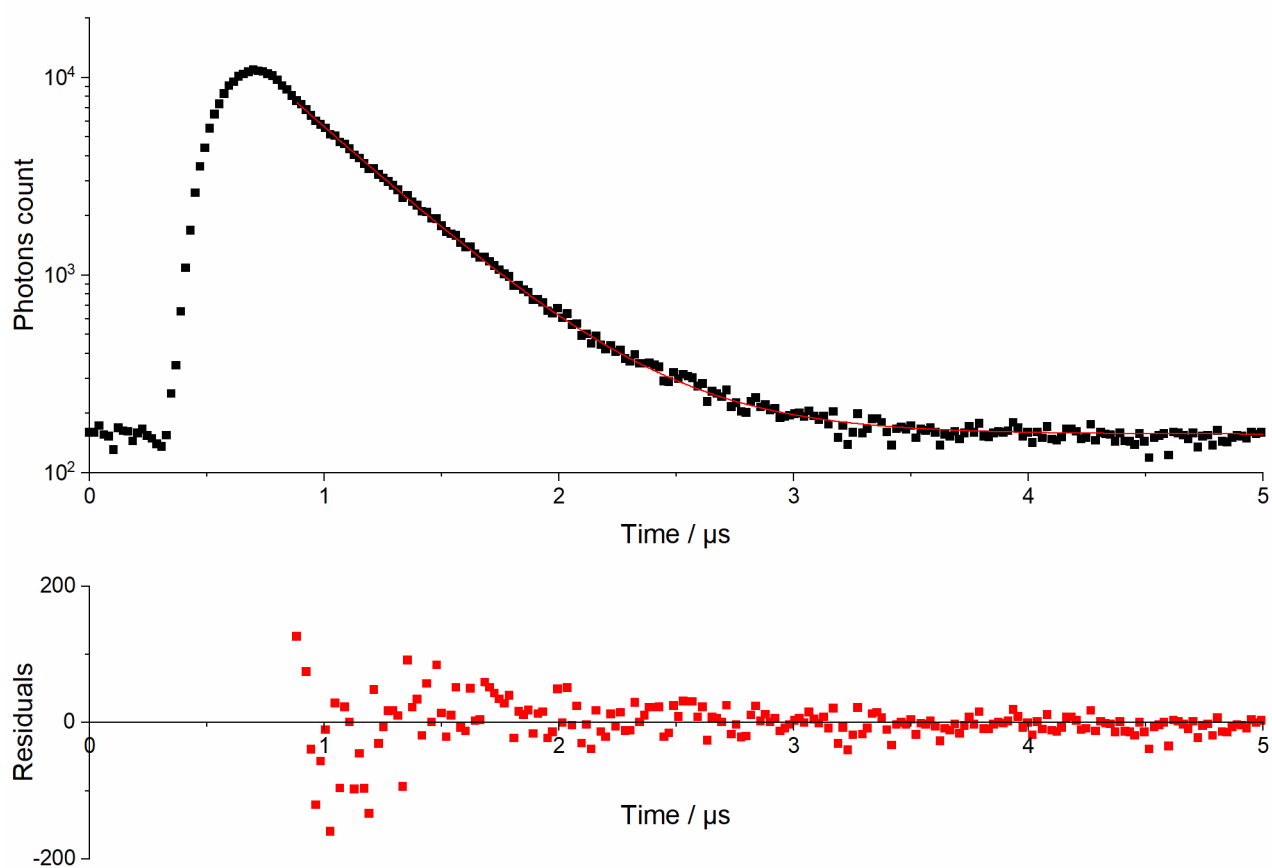


**Figure S4.** Integrated emission decay profile of  $((n\text{-C}_4\text{H}_9)_4\text{N})_2[\text{W}_6\text{I}_{14}]$  in aerated  $\text{CH}_3\text{CN}$

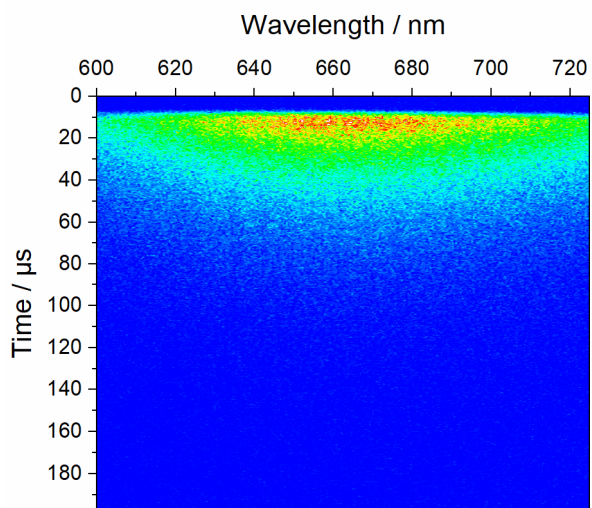


Figure S5. Emission decay map of  $((n\text{-C}_4\text{H}_9)_4\text{N})_2[\text{W}_6\text{I}_{14}]$  in deaerated  $\text{CH}_3\text{CN}$

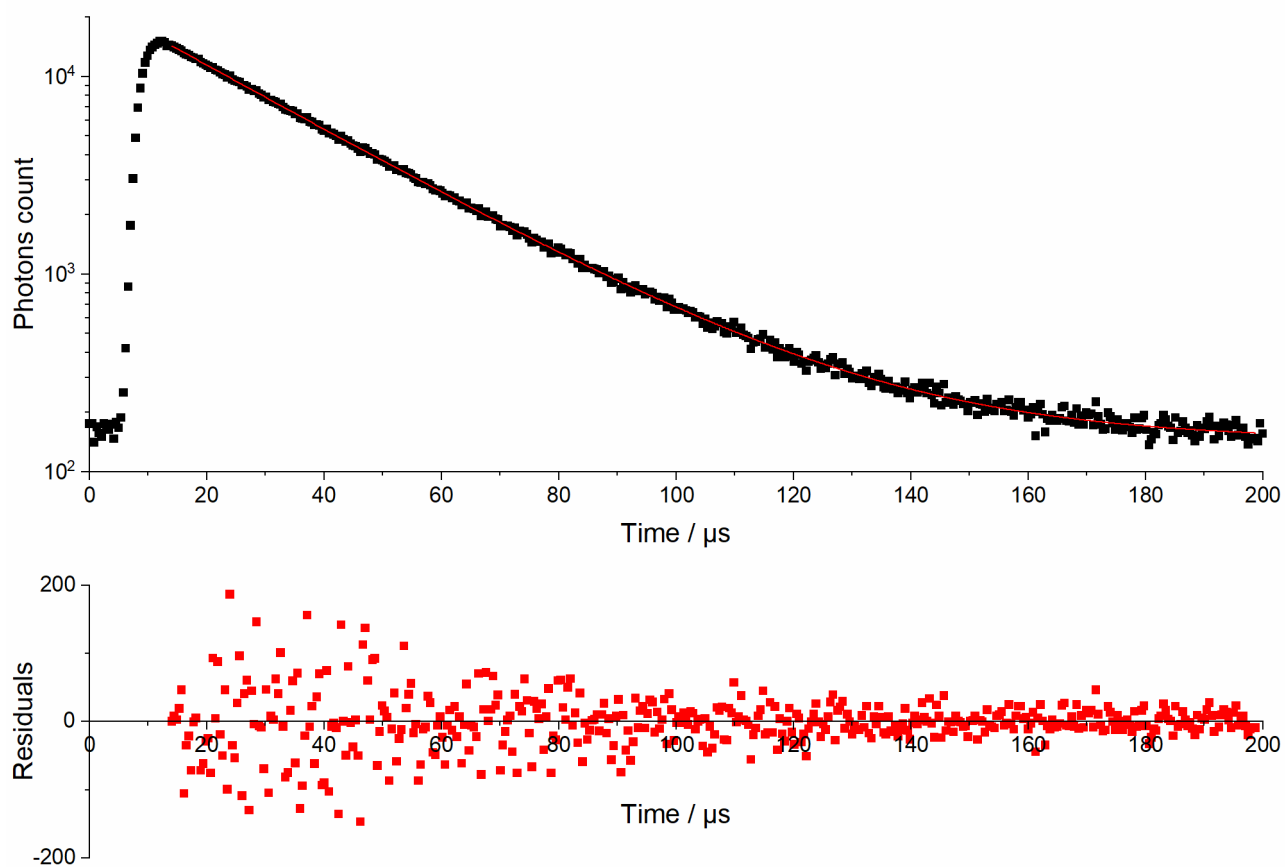
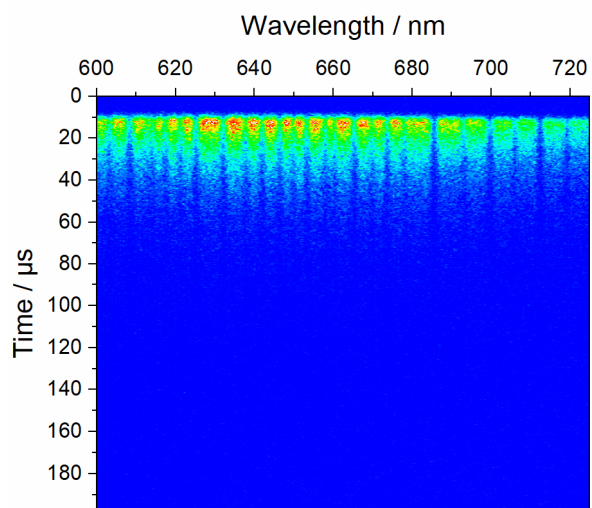
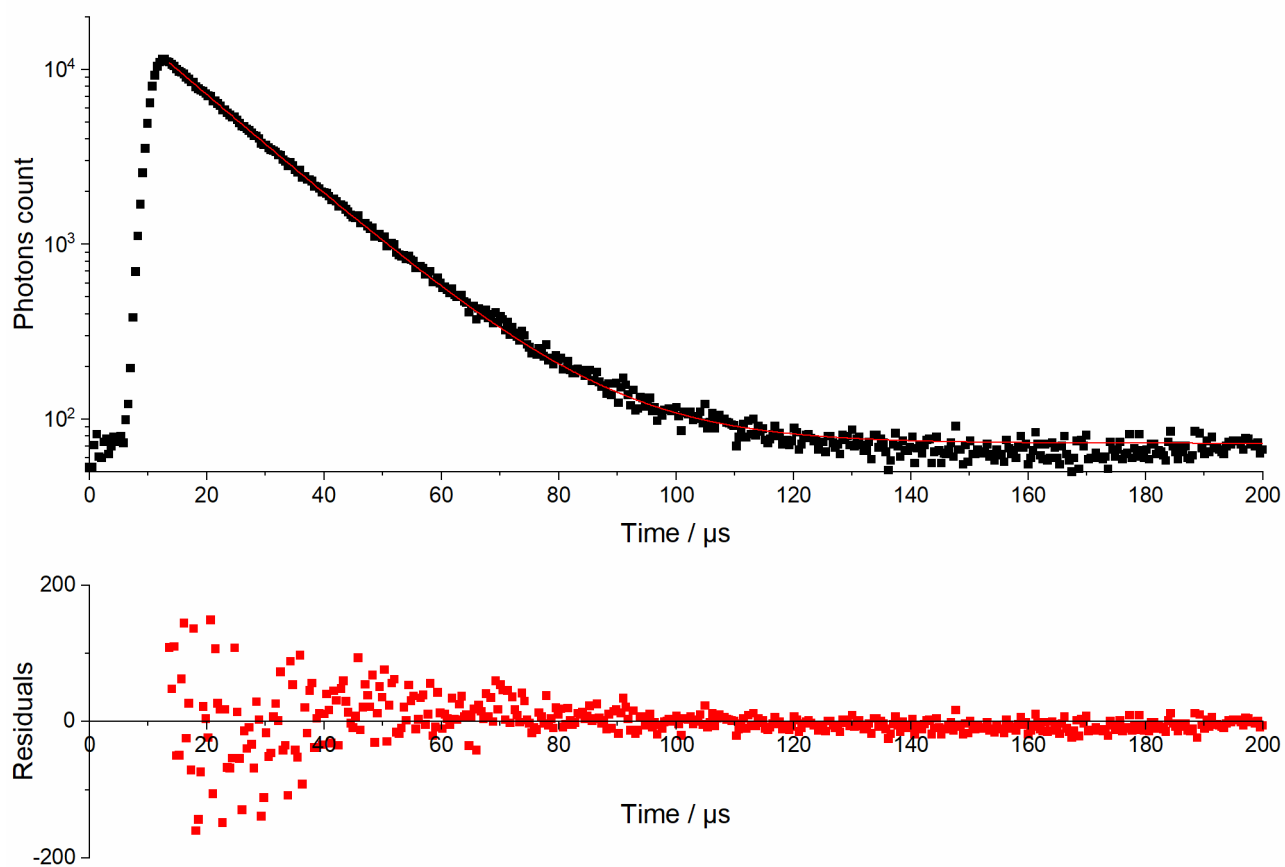


Figure S6. Integrated emission decay profile of  $((n\text{-C}_4\text{H}_9)_4\text{N})_2[\text{W}_6\text{I}_{14}]$  in deaerated  $\text{CH}_3\text{CN}$



**Figure S7.** Emission decay map of  $((n\text{-C}_4\text{H}_9)_4\text{N})_2[\text{W}_6\text{I}_{14}]$  in the solid state



**Figure S8.** Integrated emission decay profile of  $((n\text{-C}_4\text{H}_9)_4\text{N})_2[\text{W}_6\text{I}_{14}]$  in the solid state

## AQY measurements

The absolute quantum yields were measured with a C9920–03 Hamamatsu system. Such system is composed by an excitation source, a monochromator, an integrating sphere and a Hamamatsu PMA12 CCD detector. Samples are prepared as follow: a tiny amount of powder is deposited inside the quartz cuvette so that the percentage of absorbed excitation light is kept around 60% (according to the manufacturer, a minimal absorption of 50% is mandatory to generate accurate results). Using such tiny amount allows all the emitted light to be collected in a  $4\pi$  solid angle inside the integrating sphere, which cannot be the case if the cuvette is fully filled in.

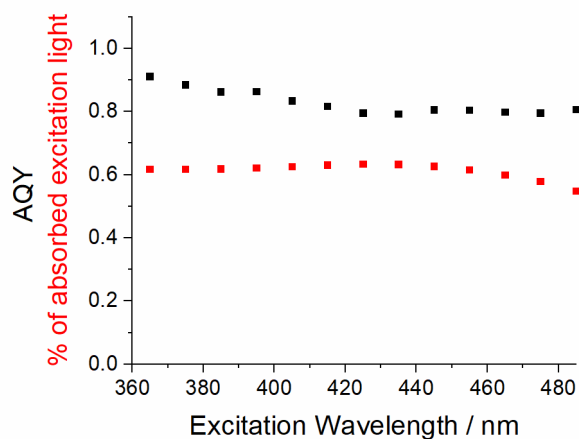


**Figure S9.** Calculated AQY values (black) and percentage of absorbed excitation light (red) used for the calculation for wavelengths ranging from 365 nm up to 485 nm. Uncertainty is around 10%.

## Two-photon emission spectra

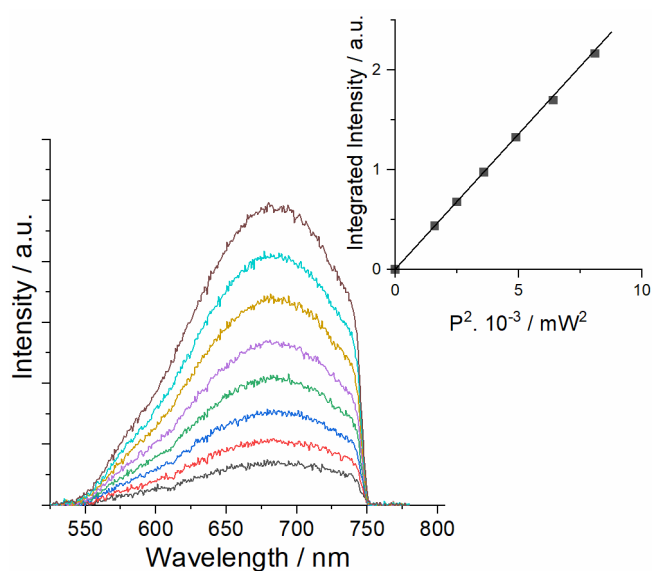


**Figure S10.** 2PE spectra vs irradiation power of a)  $((n\text{-C}_4\text{H}_9)_4\text{N})_2[\text{W}_6\text{I}_{14}]$  in deaerated  $\text{CH}_3\text{CN}$  (spectra are cut at 750 nm because of the optical filter used to prevent detector damages); inset: quadratic relationship of the observed two-photon emission intensity with the excitation laser power at 850 nm.

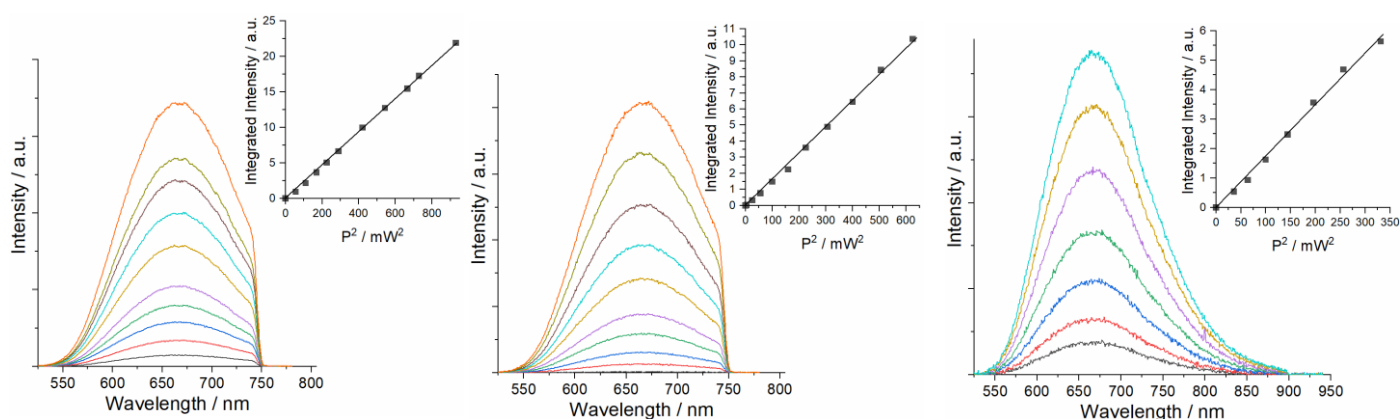


**Figure S11.** 2PE spectra vs irradiation power of  $((n\text{-C}_4\text{H}_9)_4\text{N})_2[\text{W}_6\text{I}_{14}]$  in the solid state (spectra are cut at 750 nm because of the optical filter used to prevent detector damages); inset: quadratic relationship of the observed two-photon emission intensity with the excitation laser power. Excitation at 810 nm (left), 950 nm (middle) and 1010 nm (right).

### Singlet oxygen generation studies

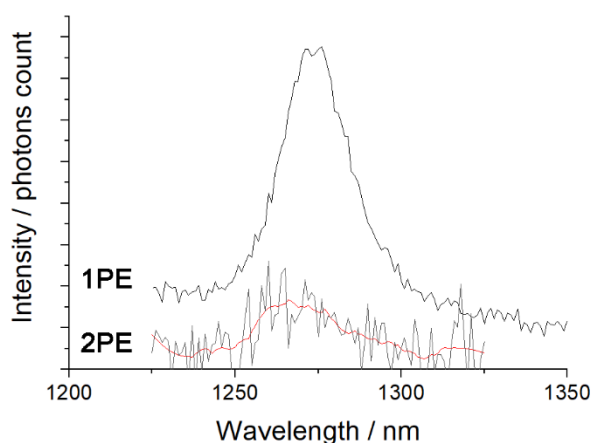


**Figure S12.** Singlet oxygen  $\text{O}_2(a^1\Delta_g)$  emission spectra observed in aerated  $\text{CH}_3\text{CN}$  upon  $((n\text{-C}_4\text{H}_9)_4\text{N})_2[\text{W}_6\text{I}_{14}]$  excitation at 375 nm (1PE) and 810 nm (2PE, the red curve is obtained by smoothing experimental data).

### References

- [1] a) J. Rodríguez-Carvajal, *Physica B* **1993**, *192*, 55-69; b) T. Roisnel, J. Rodríguez-Carvajal, *Mater. Sci. Forum* **2001**, *378-381*, 118-123.
- [2] O. S. Finikova, T. Troxler, A. Senes, W. F. DeGrado, R. M. Hochstrasser, S. A. Vinogradov, *J. Phys. Chem. A* **2007**, *111*, 6977-6990.
- [3] N. S. Makarov, M. Drobizhev, A. Rebane, *Opt. Express* **2008**, *16*, 4029-4047.
- [4] V. Kolesnichenko, L. Messerle, *Inorg. Chem.* **1998**, *37*, 3660-3663.
- [5] R. D. Hogue, R. E. McCarley, *Inorg. Chem.* **1970**, *9*, 1354-1360.
- [6] M. N. Sokolov, K. A. Brylev, P. A. Abramov, M. R. Gallyamov, I. N. Novozhilov, N. Kitamura, M. A. Mikhaylov, *Eur. J. Inorg. Chem.* **2017**, *2017*, 4131-4137.
- [7] T. C. Zietlow, D. G. Nocera, H. B. Gray, *Inorg. Chem.* **1986**, *25*, 1351-1353.
- [8] L. Riehl, A. Seyboldt, M. Ströbele, D. Enseling, T. Jüstel, M. Westberg, P. R. Ogilby, H. J. Meyer, *Dalton Trans* **2016**, *45*, 15500.